



Glioblastoma Proximity to the Lateral Ventricle Alters Neurogenic Cell Populations of the Subventricular Zone

Luisina B. Ripari^{1†}, Emily S. Norton^{2,3,4†}, Raquel Bodoque-Villar⁵, Stephanie Jeanneret^{2,6}, Montserrat Lara-Velazquez², Anna Carrano², Natanael Zarco², Carla A. Vazquez-Ramos², Alfredo Quiñones-Hinojosa², Carlos de la Rosa-Prieto^{1*} and Hugo Guerrero-Cázares^{2*}

OPEN ACCESS

Edited by:

Sunit Das,
St. Michael's Hospital, Canada

Reviewed by:

Catalina Lee-Chang,
Northwestern University,
United States

Rebecca Ihrie,

Vanderbilt University, United States

*Correspondence:

Carlos de la Rosa-Prieto
Carlos.delarosa@uclm.es

Hugo Guerrero-Cázares
Guerrero-Cazares.Hugo@mayo.edu

[†]These authors have contributed
equally to this work

Specialty section:

This article was submitted to
Neuro-Oncology and
Neurosurgical Oncology,
a section of the journal
Frontiers in Oncology

Received: 06 January 2021

Accepted: 07 June 2021

Published: 29 June 2021

Citation:

Ripari LB, Norton ES,
Bodoque-Villar R, Jeanneret S,
Lara-Velazquez M, Carrano A,
Zarco N, Vazquez-Ramos CA,
Quiñones-Hinojosa A,
de la Rosa-Prieto C and
Guerrero-Cázares H (2021)
Glioblastoma Proximity to the
Lateral Ventricle Alters
Neurogenic Cell Populations
of the Subventricular Zone.
Front. Oncol. 11:650316.
doi: 10.3389/fonc.2021.650316

¹ Department of Medical Sciences, Facultad de Medicina de Albacete, Universidad de Castilla-La Mancha, Albacete, Spain,

² Department of Neurosurgery, Mayo Clinic, Jacksonville, FL, United States, ³ Neuroscience Graduate Program, Mayo Clinic Graduate School of Biomedical Sciences, Jacksonville, FL, United States, ⁴ Regenerative Sciences Training Program, Center for Regenerative Medicine, Mayo Clinic, Jacksonville, FL, United States, ⁵ Translational Research Unit, Hospital General Universitario de Ciudad Real, Ciudad Real, Spain, ⁶ Faculty of Psychology and Sciences of Education, University of Geneva, Geneva, Switzerland

Despite current strategies combining surgery, radiation, and chemotherapy, glioblastoma (GBM) is the most common and aggressive malignant primary brain tumor in adults. Tumor location plays a key role in the prognosis of patients, with GBM tumors located in close proximity to the lateral ventricles (LVs) resulting in worse survival expectancy and higher incidence of distal recurrence. Though the reason for worse prognosis in these patients remains unknown, it may be due to proximity to the subventricular zone (SVZ) neurogenic niche contained within the lateral wall of the LVs. We present a novel rodent model to analyze the bidirectional signaling between GBM tumors and cells contained within the SVZ. Patient-derived GBM cells expressing GFP and luciferase were engrafted at locations proximal, intermediate, and distal to the LVs in immunosuppressed mice. Mice were either sacrificed after 4 weeks for immunohistochemical analysis of the tumor and SVZ or maintained for survival analysis. Analysis of the GFP+ tumor bulk revealed that GBM tumors proximal to the LV show increased levels of proliferation and tumor growth than LV-distal counterparts and is accompanied by decreased median survival. Conversely, numbers of innate proliferative cells, neural stem cells (NSCs), migratory cells and progenitors contained within the SVZ are decreased as a result of GBM proximity to the LV. These results indicate that our rodent model is able to accurately recapitulate several of the clinical aspects of LV-associated GBM, including increased tumor growth and decreased median survival. Additionally, we have found the neurogenic and cell division process of the SVZ in these adult mice is negatively influenced according to the presence and proximity of the tumor mass. This model will be invaluable for further investigation into the bidirectional signaling between GBM and the neurogenic cell populations of the SVZ.

Keywords: glioblastoma, subventricular zone (SVZ), lateral ventricle, neural stem cell (NSC), cancer stem cell (CSC), neurogenic niche

INTRODUCTION

Glioblastoma (GBM) is the most frequent and aggressive type of malignant primary brain tumor in adults (1, 2). Patients suffering from GBM have a median survival of approximately 15 months despite advanced therapeutic strategies of combinatorial surgery, chemotherapy, and radiation (3, 4). Interestingly, tumor progression for GBM patients is greatly affected by tumor location. Lateral ventricles (LVs) infiltrating tumors account for over 50% of all GBM patients (5). These LV-contacting tumors result in higher incidence of distant recurrence, as well as larger tumor volume and worse survival expectancy in patients (6–9). Furthermore, GBM patients who receive radiotherapy that includes the ventricular wall ipsilateral to the tumor show increased survival when compared to patients where the ipsilateral ventricular wall is avoided (10), indicating the involvement of LV-derived factors in GBM progression.

The reason for worse patient outcome in these cases is unknown, though could be due in part to contact with the subventricular zone (SVZ) present in the lateral wall of the LV. The SVZ is the largest stem cell niche in the mammalian adult brain, including humans (11–14). In rodents, neural stem cells (NSCs) of the SVZ form new neurons and glia throughout life, differentiating to neuroblasts or glial progenitors that then migrate to their site of terminal differentiation (15–18). Studies have shown a high amount of similarity in the biology of NSCs and stem-like GBM cells, including shared pathways of self-renewal, differentiation, and cell migration (19, 20). Additionally, several studies have identified NSCs of the SVZ as a potential cell-of-origin for GBM, pointing to the potential involvement of NSCs in GBM progression (21–25).

Shared mechanisms between NSCs and GBM support the idea that stem cell-supportive factors contained within the SVZ support the proliferation and stemness of LV-proximal tumors. This may include a bidirectional crosstalk between NSCs/progenitors and GBM cells that leads to changes in SVZ biology and patient outcome. Previous work has shown that cell types within the SVZ, including NSCs and their progeny, are altered in response to GBM in rodents (26). Here, we develop a novel rodent model of LV-proximal GBM and examine the reciprocal relationship between the SVZ and GBM tumors. We particularly focused on cell population and proliferation changes in the SVZ as a consequence of GBM proximity to the LV.

MATERIALS AND METHODS

Experimental Animals

All *in vivo* experiments were approved by the Institutional Animal Care and Use Committee of Mayo Clinic. Mice were housed in a fully AALAC-accredited facility in accordance with all federal and local regulations. Male athymic immunosuppressed J:NU mice (The Jackson Laboratory, strain 007850) were maintained at Mayo Clinic Jacksonville with a 12-hour light-dark cycle and *ad libitum* feeding. Animals were utilized for experiments at an age between 6–8 weeks.

Primary GBM Cell Xenograft and Euthanasia

We utilized a primary cell line of human GBM cells (GBM1A, also known as line 020913) (27). GBM1A cells were transduced with a GFP-luciferase lentivirus (RediFect™ Red-FLuc-GFP, Perkin Elmer CLS960003) and sorted for GFP positivity. Following cell transduction, intracranial implantation of tumors was performed as previously described (28–31). Briefly, mice were anesthetized and placed in a stereotactic frame. 5.0×10^5 GBM1A-GFP luciferase+ cells were injected in 2 μ L of DMEM/F12 into the right brain hemisphere. 3 injection sites were established in the following coordinates (in mm relative to bregma); LV-proximal: AP: 1.0, L: 1.2, D: 2.3, n = 17; LV-intermediate: AP: 1.5, L: 1.3, D: 3, n = 7; and LV-distal: AP: 1.0, L: 2.1, D: 2.3, n = 17. Tumor growth was monitored weekly by bioluminescence following luciferin injection. For survival experiments, mice were maintained until reaching humane endpoint criteria following GBM xenograft. For histology analysis, mice were maintained for 4 weeks after tumor implantation (n=7). Mice were then anesthetized and perfused with 4% paraformaldehyde. Brains were extracted and cryoprotected in 30% sucrose. Brains were sectioned using an HM 430 Freezing Microtome at 30 μ m thickness. Sections were stored in 30% ethylene glycol, 20% glycerol, 0.05M PBS, pH 7.4 at -20°C until immunohistochemical processing.

Immunohistochemistry

Sections were permeabilized with 0.1% Triton in PBS (PBST) and blocked with 1% BSA and 10% normal horse serum. In the case of caspase-3 and Ki67 staining, antigen retrieval was performed using sodium citrate buffer (10 mM + 0.05% Tween) at 90°C for 25 minutes, followed by cooling in the sodium citrate buffer for 30 minutes before washing and blocking. Sections were then incubated overnight at 4°C in primary antibody at various concentrations (**Table 1**) diluted in 0.2% normal horse serum in PBST. Sections were washed and incubated in the dark for 1 hour at room temperature with secondary antibodies (**Table 2**) at a concentration of 1:500 in 2% normal horse serum in PBST. Sections were washed and counterstained with DAPI as a nuclear dye. At least three sections per animal were used per staining condition.

Imaging

Immunohistochemical preparations were visualized using a confocal microscope (Zeiss LSM800). Tumors were visualized by GFP+ cells and imaged with 10X, 25X, 40X or 63X objectives. ZEN® Blue Edition software (Zeiss) was then used to process the image. All sections for the same antibody combinations were imaged in the same way using the same exposure levels.

Volumetric Analysis

Tumor area data was obtained using ZEN® Blue Edition software. GFP+ tumors were traced using the “Draw Spline Contour” tool in ZEN software to obtain the area of each tumor section. Morphometric volume was then calculated

TABLE 1 | Primary antibodies used.

Antibody	Species	Detection	Dilution Factor	Catalog
GFP	Mouse	GFP+ GBM cells	1:500	Abcam (ab1218)
Human Nuclei (HuNu)	Mouse	Human GBM cells	1:200	Millipore (MAB1281)
Ki67	Rabbit	Proliferating cells	1:200	Thermo (RM-9106-S0)
	Mouse			Novocastra (NCL-L-Ki67-MM1)
phosphohistone H3 (pH3)	Rabbit	Proliferating cells	1:200	Cell Signaling (9701S)
GFAP	Rabbit	Astrocytic cells	1:200	Dako (Z0334)
SOX2	Rat	Undifferentiated cells	1:500	Thermo (14-9811-82)
OLIG2	Rabbit	Oligodendrocyte precursors	1:500	Millipore (AB9610)
Cleaved caspase-3 (Asp175)	Rabbit	Apoptotic cells	1:200	Cell Signaling (9661)
Doublecortin (DCX)	Goat	Neuroblasts	1:200	Santa Cruz (SC-8066)

TABLE 2 | Secondary antibodies used.

Secondary Antibody Wavelength	Species and Reactivity	Dilution Factor	Catalog
Alexa Fluor 568	Donkey anti-rabbit	1:500	Invitrogen (A10042)
Alexa Fluor 647	Chicken anti-rabbit	1:500	Invitrogen (A21443)
Alexa Fluor 488	Donkey anti-goat	1:500	Invitrogen (10246392)
Alexa Fluor 555	Donkey anti-mouse	1:500	Invitrogen (A31570)
Alexa Fluor 594	Donkey anti-rat	1:500	Invitrogen (A21209)

using the Cavalieri principle, which allows an accurate estimation of the volume (V) of a structure independently of its shape and size (32). This is calculated by finding surface area (A) of a number (n) of parallel sections spaced at a constant distance (t) and inserting into the following equation: $V = t * (A_1 + A_2 + A_3... + A_n)$.

Cell Quantification

ZEN[®] Blue software was used to estimate the number of cells expressing the human nucleus marker, HuNu, and the proliferation marker, Ki67 in the different groups, both in the tumor as in SVZ. In addition, cells positive for cleaved caspase-3, phosphohistone H3, SOX2, SOX2/GFAP, DCX and OLIG2 present in SVZ were quantified. For cell quantification of the SVZ, the ipsilateral and contralateral SVZ were imaged in 20X tiles using a confocal microscope. Using the ZEN[®] Blue software, the SVZ region was manually traced using the “Draw Spline Contour” tool to specifically isolate the cells of the SVZ for the subsequent analysis. Signal background was removed by adjusting the channel histogram to the peak of the curve and remaining cells were considered positive and counted. Cell quantification was performed from planes with no tumor cell presence in order to avoid changes in cell proportion. The cell density (number of cells per square millimeter) was calculated for each image.

Statistical Analysis

All data is represented as the mean \pm the standard error (SEM) unless otherwise indicated. Statistical analysis and graphical representation were performed using GraphPad Prism[®] 6 software. Normal distribution of data was assessed using the Shapiro-Wilk normality test. To compare among multiple groups, analysis of variance (ANOVA) with Tukey’s post-hoc correction was performed. For independent comparisons

between two groups the student’s t-test was performed. The level of significance was determined as $p < 0.05$.

RESULTS

GBM Proximity to the LV Contributes to Tumor Growth and Survival Outcome

We first evaluated the effect of the LV proximity to tumor growth in our animal model. Patient-derived GBM cells transduced to express GFP and luciferase were implanted at locations proximal, intermediate, and distal to the LV (**Figure 1A** and **Supplementary Figure 1**). Following a 4-week period, tumors were evaluated for volume, cellular density, proliferation, and apoptosis. When tumors were injected into locations proximal and intermediate to the LV, we observed a trend towards increased tumor volume compared to LV-distal tumors (LV-proximal: 2.55 mm³; LV-intermediate: 3.74 mm³; LV-Distal: 1.19 mm³; **Figure 1B**) with no difference in tumor cell density (**Supplemental Figure 2**). In order to determine whether LV proximity induced differences in proliferation or apoptosis, we performed immunofluorescence staining for Ki67, cleaved caspase-3, and human nuclei (HuNu)+ GBM cells. In tumors injected in LV-proximal and LV-intermediate locations we observed a significantly higher percentage of Ki67+/HuNu+ GBM cells than in LV-distal tumors (LV-proximal: 23.36%, LV-Intermediate: 23.48%, LV-Distal: 11.41%; **Figures 1C–F**), indicating an increase in GBM proliferative index dependent on proximity to the LV. Additionally, the percentage of cleaved caspase-3+/HuNu+ cells was significantly decreased in LV-intermediate tumors compared to LV-proximal tumors (LV-Proximal: 0.014%, LV-Intermediate: 0.0037%, LV-Distal: 0.015%; **Figures 1G–J**).

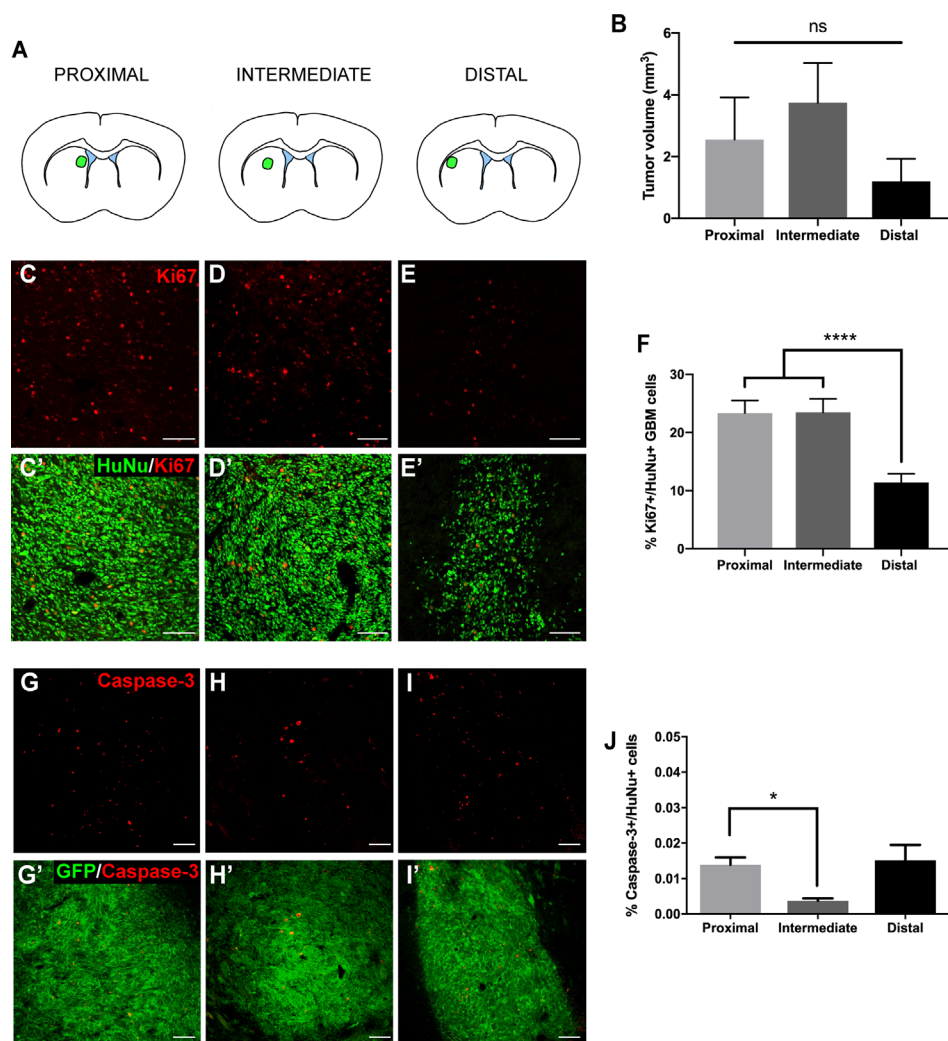


FIGURE 1 | GBM proximity to the lateral ventricle induces increased tumor growth. **(A)** Schematic illustration of the LV-proximal, LV-intermediate, and LV-distal injection sites. **(B)** Quantification of GFP+ tumor volume in LV-proximal (n = 6), LV-intermediate (n = 5), and LV-distal (n = 5) groups. **(C–E)** Representative Ki67 immunohistochemical staining in **(C)** LV-proximal, **(D)** LV-intermediate, and **(E)** LV-distal GBM. Merged with HuNu staining (green, C'–E'). Scale bar = 100 μ m. **(F)** Quantification of the percentage of Ki67+/HuNu+ cells within the GBM tumor between LV-proximal (n = 6), LV-intermediate (n = 5), and LV-distal (n = 5) groups. **(G–I)** Representative cleaved caspase-3 (cleaved C3) immunohistochemical staining in **(G)** LV-proximal, **(H)** LV-intermediate, and **(I)** LV-distal GBM. Merged with GFP staining (green, G'–I'). Scale bar = 100 μ m. **(J)** Quantification of the percentage of cleaved caspase-3+/HuNu+ cells in the GBM tumor between LV-proximal (n = 7), LV-intermediate (n = 3), and LV-distal (n = 5) groups. The data are presented as mean \pm SEM. * $p < 0.05$, **** $p < 0.0001$. NS, not significant.

We then evaluated the differences in tumor growth *via* bioluminescence imaging (BLI) and long-term survival outcome. Due to similar Ki67+ staining in LV-proximal and LV-intermediate tumor locations, we only used the LV-proximal tumor site for survival analysis. Tumor growth measured by increase in total flux (photons per second) was significantly higher in LV-proximal tumors than LV-distal tumors at 5 weeks post-xenograft (**Figures 2A, B**). Additionally, mice with LV-proximal tumors exhibited decreased median survival compared to their LV-distal tumor-bearing counterparts (LV-Proximal: 36 days, LV-Distal 52 days; **Figure 2C**). These findings show that we are able to effectively model several of the clinical differences of LV-proximal GBM compared to LV-distal GBM,

such as increased tumor burden and decreased survival, in an immunocompromised rodent model.

Proliferation Levels in GFP-/HuNu- Cells Within the SVZ Are Decreased as a Result of GBM Tumor Proximity

The LV contains the SVZ, the largest neurogenic niche in mammals (11–14). Previous studies have indicated that the cellular populations of the SVZ are altered due to the presence of GBM (26), but do not explore the effect of tumor proximity on different neurogenic cell populations. We observed that SVZ size was not altered by the presence of tumors when compared between groups and between sides ipsilateral and contralateral

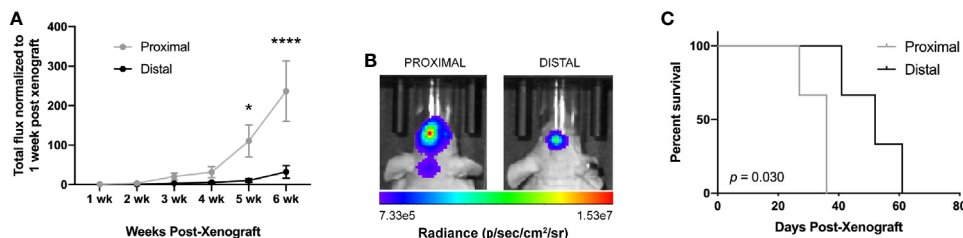


FIGURE 2 | GBM proximity to the lateral ventricles impacts long-term outcome in rodents. **(A)** Quantification of BLI total flux fold change over time in the LV-proximal and LV-distal GBM tumor conditions ($n = 7$). **(B)** Representative BLI images in radiance (photons/second/centimeter/steradian) of immunosuppressed athymic nude mice bearing orthotopic patient-derived GBM at LV-proximal (left) and LV-distal (right) locations at five weeks post injection. **(C)** Kaplan-Meier survival curve of mice bearing tumors in LV-proximal and LV-distal sites ($n = 3$). The median survival for LV-proximal or LV-distal tumor bearing mice were 36 and 52 days, respectively. The data are presented as mean \pm SEM. * $p < 0.05$, **** $p < 0.0001$.

to the tumor (data not shown). To explore the effect of GBM proximity on mouse SVZ cell proliferation, we performed immunostaining for Ki67 and evaluated Ki67+/GFP-/HuNu-cells in the regions of the SVZ where the tumor growth was also present, in both ipsilateral and contralateral hemispheres. We determined that the proliferation rate of innate cells in the SVZ ipsilateral to the tumor site is significantly decreased compared to the contralateral SVZ in the presence of LV-proximal and LV-intermediate GBM, but not in LV-distal GBM (LV-proximal: 14.01 cells/mm² ipsilateral vs. 40.97 cells/mm² contralateral; LV-intermediate: 15.85 cells/mm² ipsilateral vs. 40.41 cells/mm² contralateral; LV-distal: 24.18 cells/mm² ipsilateral vs. 50.60 cells/mm² contralateral; **Figures 3A–G**), indicating that tumor proximity decreases SVZ cell proliferation.

To verify that SVZ cells have decreased levels of mitosis with increased tumor proximity, we also performed IHC for phosphohistone H3 (pH3), a marker of chromatin condensation with higher specificity for mitosis than Ki67. Again, we determined that the proliferation rate of HuNu-cells in the SVZ ipsilateral to the LV-proximal tumor is significantly decreased compared to the contralateral hemisphere (LV-proximal: 92.51 cells/mm² ipsilateral vs. 182.93 cells/mm² contralateral; **Supplemental Figures 3A–E**). In contrast, there was no decrease in the proliferation of the ipsilateral SVZ cells in LV-distal GBM when compared to the contralateral SVZ (LV-distal: 233.62 cells/mm² ipsilateral vs. 214.67 cells/mm² contralateral; **Supplemental Figures 3A–E**). Despite changes in proliferation, almost no cleaved caspase-3 labeling was seen in GFP- cells of the SVZ (data not shown). These findings further support a shift in the proportion of SVZ cell proliferation in response to tumor proximity.

SOX2+/GFAP+/HuNu- Cells Within the SVZ Are Decreased as a Result of GBM Tumor Proximity

The SVZ contains NSCs that differentiate into progenitor cells, ultimately leading to the production of new neurons and glia throughout life (15–18). To examine how tumor proximity affects these populations of cells, we performed immunohistochemical staining for a variety of markers of different neurogenic cell types. We evaluated the staining for

SOX2, a marker of NSCs and progenitors (33), in response to tumor proximity. SOX2+/HuNu- cell density is significantly decreased in the ipsilateral SVZ of LV-proximal tumors compared to LV-intermediate and LV-distal tumors (LV-proximal: 1273.83 cells/mm²; LV-intermediate: 2706.12 cells/mm²; LV-distal: 2853.37 cells/mm²; **Figures 4A–D**). Cells that are positive for both GFAP and SOX2 and negative for HuNu, that represent astrocytic NSCs of the SVZ (34), were also decreased in response to LV-proximal tumors compared to LV-intermediate and LV-distal tumors (LV-proximal: 393.20 cells/mm²; LV-intermediate: 604.48 cells/mm²; LV-distal: 673.43 cells/mm²; **Figures 4E–H**), showing that there is a decrease in NSCs and progenitors in the SVZ in response to LV-proximal tumors.

GBM Proximity to the Lateral Ventricle Decreases Oligodendrocyte Precursor and Neuroblast Density in the SVZ

To examine changes in neurogenic progeny in the SVZ, we also analyzed the number of GFP-/oligodendrocyte precursor cells (OPCs) and neuroblasts in relation to GBM tumor proximity. The differentiation of NSCs to OPCs is accompanied by the expression of the transcription factor OLIG2. We found that the presence of GBM significantly decreases the number of GFP-/OLIG2+ cells in the ipsilateral SVZ compared to the contralateral SVZ among all groups (ipsilateral 261.95 cells/mm² vs. contralateral 353.96 cells/mm²; **Figure 5A**). Additionally, there are significantly fewer GFP-/OLIG2+ cells in the ipsilateral SVZ of LV-proximal group than in the LV-intermediate or LV-distal groups (LV-proximal: 159.88 cells/mm²; LV-intermediate: 339.27 cells/mm²; LV-distal: 386.19 cells/mm²; **Figures 5B–E**), indicating that GBM proximity to the SVZ significantly decreases OPC generation in the SVZ.

The differentiation of NSCs into neuroblasts, as well as their migration through the brain and incorporation into the olfactory bulb, is well-studied in rodents (16, 35). Previous studies have shown an increase in the levels of SVZ neuroblasts in the presence of GBM, as well as neuroblast migration to the tumor site (26). In order to examine how the neuroblast population was changed in response to tumor proximity to the SVZ, we performed immunohistochemical staining for doublecortin (DCX+), a widely used marker for migratory neuroblasts.

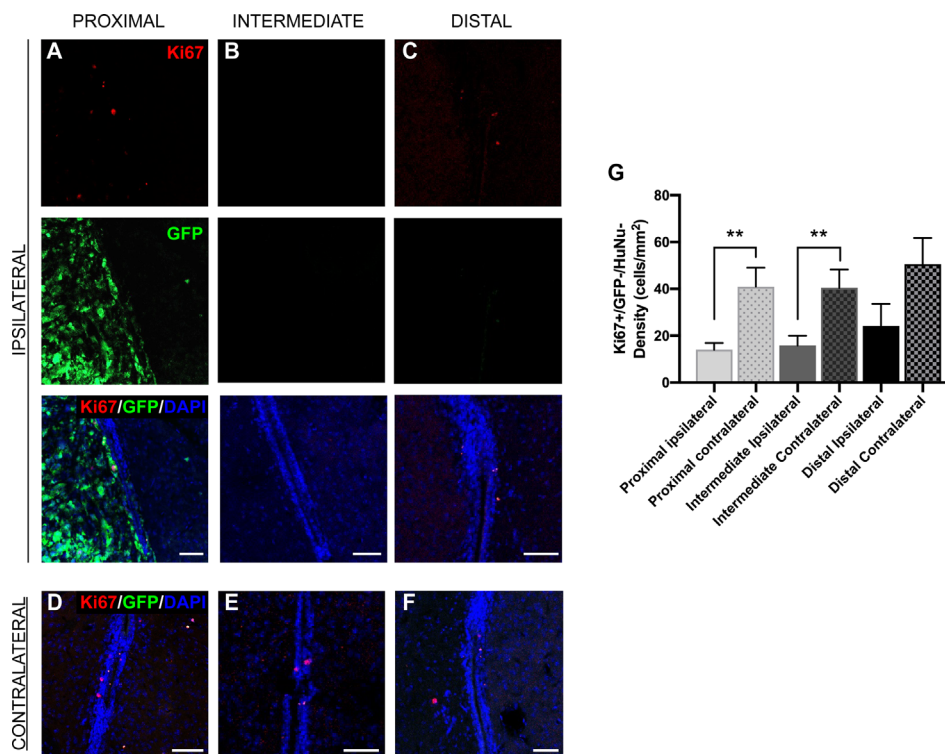


FIGURE 3 | GBM proximity to the LV negatively influences Ki67 expression in the SVZ. **(A–F)** Representative images of immunohistochemical staining for Ki67 in GFP-cells of the SVZ **(A–C)** ipsilateral and **(D–F)** contralateral to the tumor. Red = Ki67, green = GFP, Blue = DAPI. This was compared between **(A, D)** LV-proximal, **(B, E)** LV-intermediate, and **(C, F)** LV-distal GBM groups. Scale bar = 50 μ m. **(G)** Quantification of Ki67+ cell density in the SVZ comparing between the SVZ ipsilateral and contralateral to the GBM in LV-proximal (n = 6), LV-intermediate (n = 5), and LV-distal (n = 5) mice. Data are presented as mean \pm SEM. ** $p < 0.01$.

Interestingly, there was no significant change in GFP-/DCX+ cells among groups when measuring in the SVZ ipsilateral to the injection site (LV-proximal: 1608.86 cells/mm²; LV-intermediate: 1936.69 cells/mm²; LV-distal: 2484.84 cells/mm²; **Supplemental Figure 4**), although there was a trend towards decreased GFP-/DCX+ cells with increased GBM proximity to the LV. These findings suggest that the proximity of GBM to the LV does not affect NSC differentiation down the neuroblast lineage, despite changes in the number and proliferation of NSCs. We did not observe any GFP-/DCX+ cells migrating to the tumor site (data not shown). While there were no significant changes in the ipsilateral hemisphere to the tumor, mice with LV-proximal tumors had significantly decreased DCX+ cells in the contralateral hemisphere than LV-intermediate conditions (LV-proximal: 1295.65 cells/mm²; LV-intermediate: 2427.31 cells/mm²; LV-distal: 1988.12 cells/mm², **Figures 6A–D**).

DISCUSSION

In this study, we highlight a two-way relationship between GBM tumors and SVZ biology dependent on tumor proximity to the LV in rodents. Our results indicate that human GBM cells respond to the LVs in a proximity-dependent manner by increasing their proliferation, ultimately resulting in decreased

survival. Furthermore, we observed that tumor proximity to the LV decreases some aspects of neurogenesis in the SVZ, including proliferation as well as the density of NSCs and progenitors.

GBM tumors are more malignant in patients when located proximal to the LV than in LV-distal counterparts. The increased malignancy is evidenced by increased tumor size, increased distal recurrence, and decreased survival independent of extent of resection (5, 6, 8, 9, 36). Our work is the first to study the proximity-dependent interaction between GBM and the SVZ in a rodent model. This model recapitulates several of the features of LV-proximal GBM in patients, including increased tumor growth, increased proliferation, and decreased survival. It remains unclear the reason for increased malignancy in these tumors. Despite previous studies describing worse prognosis in patients with GBM close to the LVs, there is no substantial evidence tying these clinical findings to a molecular signature of GBM. Although some studies have linked LV-proximal GBM to characteristics such as molecular subtype and the expression of stem cell markers, others have found no association of LV-proximal GBM with a molecular signature (37–39). This may indicate that the increased malignancy of LV-proximal GBM may not be a cell-intrinsic factor, but a product of the SVZ microenvironment. This is supported by our previous studies as well as this work, where tumors derived from the same cell line become more malignant in response to the LV microenvironment.

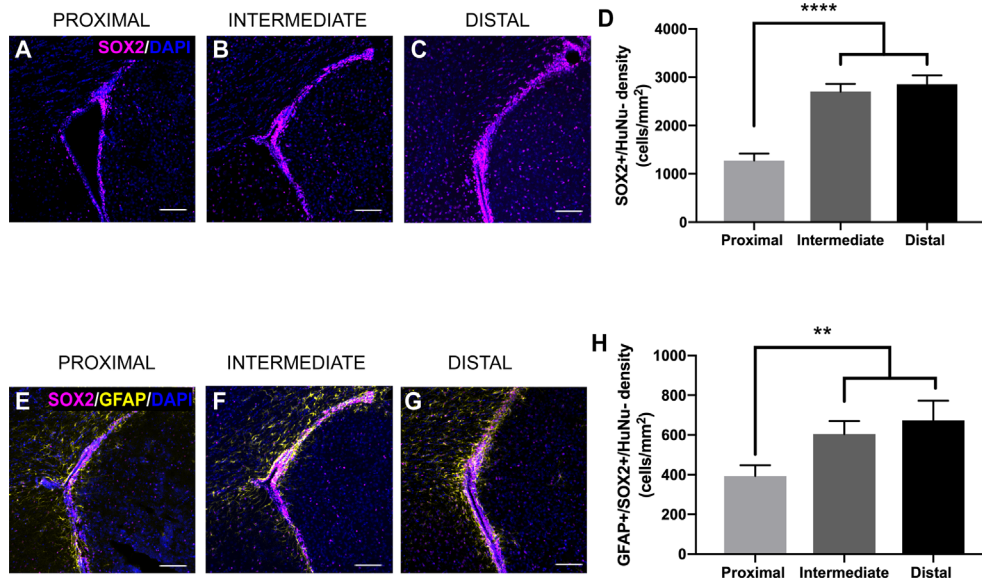


FIGURE 4 | SVZ SOX2+ progenitor number is altered by LV-proximal GBM. **(A–C)** Representative images of SOX2+ cells in the GFP-/HuNu- cells of the SVZ in **(A)** LV-proximal, **(B)** LV-intermediate, and **(C)** LV-distal groups. Scale bar = 100 μ m. **(D)** Quantification of SOX2+ cell density in the SVZ of LV-proximal, LV-intermediate, and LV-distal GBM mice. **(E–G)** Representative images of GFAP+/SOX2+ cells in the SVZ of **(E)** LV-proximal, **(F)** LV-intermediate, and **(G)** LV-distal groups. Scale bar = 100 μ m. **(H)** Quantification of GFAP+/SOX2+ cell density in the SVZ of LV-proximal (n = 7), LV-intermediate (n = 5), and LV-distal (n = 5) GBM mice. Data are presented as mean \pm SEM. ***p* < 0.01, *****p* < 0.0001.

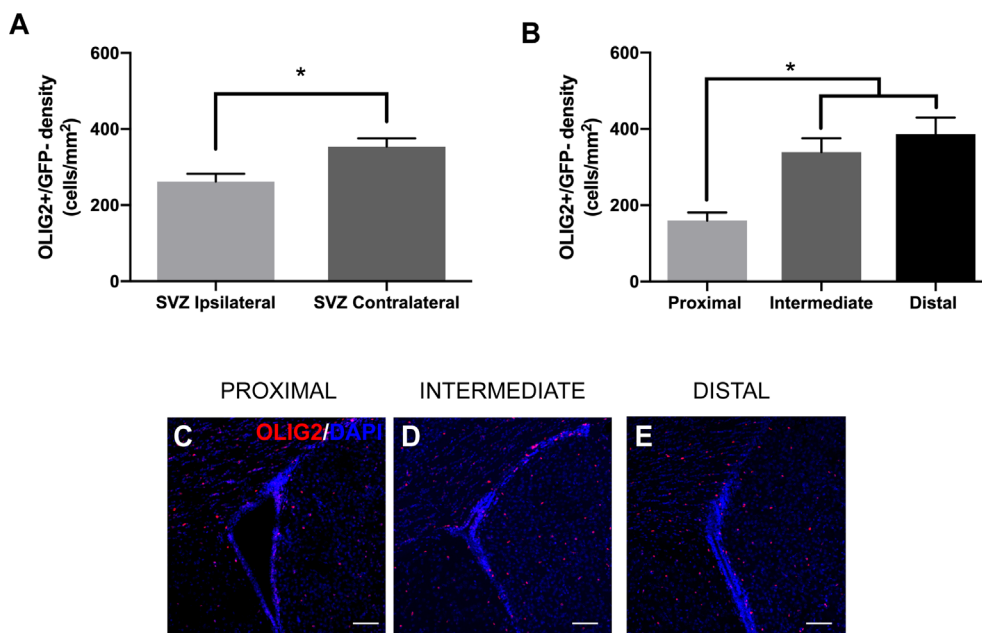


FIGURE 5 | LV-proximal GBM reduces the number of OLIG2+ progeny in the ipsilateral SVZ. **(A)** Quantification of OLIG2+ cell density in the ipsilateral and contralateral SVZ of all groups. **(B)** Quantification of OLIG2+ cell density in the SVZ ipsilateral to the tumor in LV-proximal, LV-intermediate, and LV-distal GBM mice. **(C–E)** Representative images of the ipsilateral SVZ in **(C)** LV-proximal (n = 7), **(D)** LV-intermediate (n = 5), and **(E)** LV-distal (n = 5) groups. Scale bar = 100 μ m. Data are represented as mean \pm SEM. **p* < 0.05.

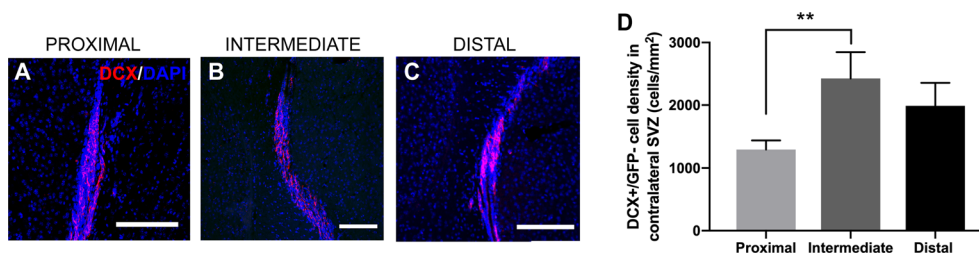


FIGURE 6 | LV-proximal GBM decreases the number of neuroblasts in the contralateral SVZ. **(A–C)** Representative images of DCX+ cells in the contralateral SVZ to the GBM in **(A)** LV-proximal ($n = 7$), **(B)** LV-intermediate ($n = 3$), and **(C)** LV-distal ($n = 5$) groups. Scale bar = 100 μm . **(D)** Quantification of DCX+ in the contralateral SVZ to the tumor between groups. Data is presented as mean \pm SEM. $**p < 0.01$.

Though this work does not identify the components responsible for increased malignancy in these tumors, there are several potential sources of neurogenesis-supporting factors that may contribute to GBM growth. The SVZ contains many NSC and progenitor cells that may interact directly with GBM cells, thereby increasing proliferation. Additionally, the SVZ contains many soluble factors which contribute to neurogenesis of SVZ NSCs that GBM cells may take advantage of. These factors may be released from the NSCs themselves or be contained within the nearby cerebrospinal fluid (CSF), ultimately contributing to GBM malignancy (40–43). Our previous work has revealed several CSF-induced transcriptomic changes in primary GBM cells, including upregulation of *SERPINA3*, *MYC*, and *SPP1* (40, 41). Gene ontology analysis has indicated an upregulation in cell viability, movement, and migration pathways induced by CSF (40), all of which may contribute to the malignancy-promoting pathways in LV-proximal tumors. These *in vitro* findings warrant the study of transcriptomic changes in SVZ and GBM cells *in vivo* using a model similar to the one presented here. The elucidation of the bidirectional mechanisms supporting GBM tumor growth requires further unbiased transcriptomic studies in both animal models and navigation-guided tumor biopsy samples.

We observed decreased proliferation of SVZ cells in the presence of LV-proximal and LV-intermediate GBM tumors compared to LV-distal tumors. These findings agree with previous work, which found decreased proliferation of SVZ cells in the presence of GBM in a syngeneic intracranial C6 rat glioma model (26). However, other studies have found that signaling from the tumor increases SVZ proliferation, resulting in hypertrophic, hypercellular areas and increased levels of stem cell markers such as Nestin (44). One potential reason for these contradictory findings is a different mechanism of interaction by GBM cells and resident SVZ cells dependent on tumor proximity to the LV. Soluble factors that are expressed by GBM, such as PDGF-A, have the ability to increase the levels of proliferation in NSCs, resulting in hypertrophic areas of the SVZ that share some features of gliomas (45, 46). However, a different effect is seen when wild-type NSCs are directly placed in co-culture with *Ink4a/Arf*^{-/-}, EGFRvIII mutated NSCs that generate tumors *in vivo* which recapitulate many features of human GBM (47, 48). Here, direct contact with glioma-like cells results in decreased levels of proliferation and increased levels of quiescence in NSCs

primarily mediated by increased Notch signaling activation (48). This suggests that GBM proximity to the LV may differentially affect resident NSCs, where LV-proximal tumors induce decreased proliferation and increased quiescence through cell-cell contact *via* Notch signaling, while LV-distal tumors may signal to NSCs primarily through secreted components.

The SVZ of mice with LV-proximal tumors have decreased neurogenic capability compared to those bearing LV-intermediate or LV-distal tumors, measured through decreased SOX2+ stem cells and progenitors, decreased SOX2+/GFAP+ NSCs, and decreased numbers of OLIG2+ cells in the ipsilateral SVZ. Though there is no significant difference in the numbers of DCX+ neuroblasts in the ipsilateral SVZ among groups, there is also a decrease in DCX+ neuroblasts in the contralateral SVZ of LV-proximal tumor mice compared to LV-intermediate tumor mice, suggesting decreased neurogenesis in the contralateral hemisphere of LV-proximal mice. Interestingly, previous data shows that GBM tumors increase neuroblast density in the SVZ (26), which differs from our present findings. SOX2+ NSCs are able to give rise to new neural cells through their multipotent potential (49). Therefore, by decreasing the number of stem cells or the rate and number of cell divisions, it is expected that we will find a lower rate of neuronal renewal in SVZ, which is a direct alteration in neurogenesis (50). Decreased neurogenesis in the ipsilateral SVZ may be due to the previously mentioned increase in NSC quiescence *via* Notch signaling through cell-cell contact. Increased quiescence of NSCs results in both decreased proliferation and decreased differentiation into progenitors (51). The decrease of neuroblasts in the contralateral hemisphere, however, may suggest the secretion of a circulating factor that is able to affect SVZ neurogenesis in the hemisphere contralateral to the tumor. The identification of factors that decrease SVZ neurogenesis secreted by GBM cells or other cells in response to the presence of GBM, such as ependymal cells or cells of the choroid plexus, need to be further explored.

Alternatively, the decrease of neuroblasts in the contralateral hemisphere may be related to decreased CSF volume or flow throughout the ventricular system without directly altering secreted factors. Neurogenesis is regulated in part by both the flow and the contained chemokines within the CSF. Both the proliferation of NSCs and the migration of newly differentiated neuroblasts down the rostral migratory stream are regulated in a flow-dependent manner (43, 52). The decrease of CSF flow and the

loss of chemokine gradient may affect neurogenesis, particularly stem cell proliferation and neuroblast migration. In support of this scenario, glioma-bearing mice have reduced CSF circulation and output compared to non-tumor controls (53), which could implicate a loss of flow-dependent regulation in GBM. The contribution of CSF flow to neurogenesis and GBM malignancy in this animal model require further studies to fully understand.

Interestingly, there are significant decreases in the level of cleaved caspase-3 labeling in the tumors LV-intermediate tumor group. GBM tumors have quite low levels of caspase-3 labeling in humans (54), so further decrease in apoptosis of the tumor may be related to increased growth. This, accompanied by increased Ki67+ GBM cells, may indicate that LV-intermediate tumors were located in a “sweet spot” where the tumors are able to take advantage of neurogenic factors contained within the SVZ niche without leading to significant neurogenic disruption. The signaling pathways between the SVZ and GBM that regulate cell proliferation and apoptosis need to be further studied in order to determine the molecular contributors to this phenomenon.

In summary, this study provides the development of a novel rodent model of LV-proximal GBM. Due to the limitations of using human cells in an immunocompromised rodent model, it will be necessary to further evaluate and validate these observations in immunocompetent murine models. The proximity of the tumor to the LV results in increased tumor proliferation, increased tumor growth, and decreased survival. Additionally, we have determined that GBM proximity to the LV also negatively impacts the number of NSCs and downstream progenitors in the SVZ. This model will be invaluable for future studies to describe the interactions between the SVZ and GBM tumors, as well as for the investigation of novel therapeutics to target signaling between these two sites. Ultimately, these findings encourage future studies to elucidate the bidirectional molecular signaling between GBM and the SVZ, particularly the identification of pathways contributing to tumor progression in LV-proximal GBM patients.

DATA AVAILABILITY STATEMENT

The raw data supporting the conclusions of this article will be made available by the authors, without undue reservation.

REFERENCES

- Lapointe S, Perry A, Butowski NA. Primary Brain Tumours in Adults. *Lancet (London England)* (2018) 392(10145):432–46. doi: 10.1016/S0140-6736(18)30990-5
- Ostrom QT, Gittleman H, Truitt G, Boscia A, Kruchko C, Barnholtz-Sloan JS. Cbtrus Statistical Report: Primary Brain and Other Central Nervous System Tumors Diagnosed in the United States in 2011–2015. *Neuro Oncol* (2018) 20 (suppl_4):iv1–iv86. doi: 10.1093/neuonc/noy131
- Koshiy M, Villano JL, Dolecek TA, Howard A, Mahmood U, Chmura SJ, et al. Improved Survival Time Trends for Glioblastoma Using the SEER 17 Population-Based Registries. *J Neuro-Oncol* (2012) 107(1):207–12. doi: 10.1007/s11060-011-0738-7
- Stupp R, Mason WP, van den Bent MJ, Weller M, Fisher B, Taphoorn MJ, et al. Radiotherapy Plus Concomitant and Adjuvant Temozolamide for

ETHICS STATEMENT

The animal study was reviewed and approved by Institutional Animal Care and Use Committee of Mayo Clinic.

AUTHOR CONTRIBUTIONS

EN, CR-P, and HG-C, conceptualized, lead the project, and analyzed the data. LR, EN, RB-V, SJ, ML-V, AC, NZ, CV-R, CR-P, and HG-C performed the experiments and analyzed the data. AQ-H performed tissue collection. HG-C provided funding. All authors contributed to the article and approved the submitted version.

FUNDING

EN was supported by the Mayo Clinic Graduate School of Biomedical Sciences, the Mayo Clinic Center for Regenerative Medicine, and the Uihlein Professorship Research Grant. ML-V was supported by CONACYT, UNAM and the Uihlein Professorship Research Grant. AQ-H was supported by the Mayo Clinic Professorship and a Clinician Investigator grant and the National Institutes of Health (NIH) (R43CA221490, R01CA200399, R01CA183827, R01CA195503, and R01CA216855). HG-C was supported by NIH grants (R03NS109444, R21CA221490, and K01NS11093001).

ACKNOWLEDGMENTS

We would like to thank Mayo Clinic Graduate School of Biomedical Sciences and the Regenerative Sciences Training Program for their support.

SUPPLEMENTARY MATERIAL

The Supplementary Material for this article can be found online at: <https://www.frontiersin.org/articles/10.3389/fonc.2021.650316/full#supplementary-material>

Glioblastoma. *N Engl J Med* (2005) 352(10):987–96. doi: 10.1056/NEJMoa043330

- Chen L, Chaichana KL, Kleinberg L, Ye X, Quinones-Hinojosa A, Redmond K. Glioblastoma Recurrence Patterns Near Neural Stem Cell Regions. *Radiother Oncol* (2015) 116(2):294–300. doi: 10.1016/j.radonc.2015.07.032
- Chaichana KL, McGirt MJ, Frazier J, Attenello F, Guerrero-Cazares H, Quinones-Hinojosa A. Relationship of Glioblastoma Multiforme to the Lateral Ventricles Predicts Survival Following Tumor Resection. *J Neuro-Oncol* (2008) 89(2):219–24. doi: 10.1007/s11060-008-9609-2
- Lim DA, Cha S, Mayo MC, Chen MH, Keles E, VandenBerg S, et al. Relationship of Glioblastoma Multiforme to Neural Stem Cell Regions Predicts Invasive and Multifocal Tumor Phenotype. *Neuro Oncol* (2007) 9 (4):424–9. doi: 10.1215/15228517-2007-023

8. Mistry AM. Clinical Correlates of Subventricular Zone-Contacting Glioblastomas: A Meta-Analysis. *J Neurosurg Sci* (2019) 63(5):581–7. doi: 10.23736/S0390-5616.17.04274-6
9. Mistry AM, Hale AT, Chambless LB, Weaver KD, Thompson RC, Ihrle RA. Influence of Glioblastoma Contact With the Lateral Ventricle on Survival: A Meta-Analysis. *J Neuro-Oncol* (2017) 131(1):125–33. doi: 10.1007/s11060-016-2278-7
10. Chen L, Guerrero-Cazares H, Ye X, Ford E, McNutt T, Kleinberg L, et al. Increased Subventricular Zone Radiation Dose Correlates With Survival in Glioblastoma Patients After Gross Total Resection. *Int J Radiat Oncol Biol Phys* (2013) 86(4):616–22. doi: 10.1016/j.ijrobp.2013.02.014
11. Gonzalez-Perez O, Quiñones-Hinojosa A. Astrocytes as Neural Stem Cells in the Adult Brain. *J Stem Cells* (2012) 7(3):181–8. doi: 10.1155/2012/378356
12. Luskin MB. Restricted Proliferation and Migration of Postnatally Generated Neurons Derived From the Forebrain Subventricular Zone. *Neuron* (1993) 11(1):173–89. doi: 10.1016/0896-6273(93)90281-U
13. Quiñones-Hinojosa A, Sanai N, Soriano-Navarro M, Gonzalez-Perez O, Mirzadeh Z, Gil-Perotin S, et al. Cellular Composition and Cytoarchitecture of the Adult Human Subventricular Zone: A Niche of Neural Stem Cells. *J Comp Neurol* (2006) 494(3):415–34. doi: 10.1002/cne.20798
14. Sanai N, Tramontin AD, Quiñones-Hinojosa A, Barbaro NM, Gupta N, Kunwar S, et al. Unique Astrocyte Ribbon in Adult Human Brain Contains Neural Stem Cells But Lacks Chain Migration. *Nature* (2004) 427(6976):740–4. doi: 10.1038/nature02301
15. Capilla-Gonzalez V, Lavell E, Quinones-Hinojosa A, Guerrero-Cazares H. Regulation of Subventricular Zone-Derived Cells Migration in the Adult Brain. *Adv Exp Med Biol* (2015) 853:1–21. doi: 10.1007/978-3-319-16537-0_1
16. Doetsch F, Alvarez-Buylla A. Network of Tangential Pathways for Neuronal Migration in Adult Mammalian Brain. *Proc Natl Acad Sci United States America* (1996) 93(25):14895–900. doi: 10.1073/pnas.93.25.14895
17. Lois C, Garcia-Verdugo JM, Alvarez-Buylla A. Chain Migration of Neuronal Precursors. *Sci (New York NY)* (1996) 271(5251):978–81. doi: 10.1126/science.271.5251.978
18. Mizrak D, Levitin HM, Delgado AC, Crotet V, Yuan J, Chaker Z, et al. Single-Cell Analysis of Regional Differences in Adult V-SVZ Neural Stem Cell Lineages. *Cell Rep* (2019) 26(2):394–406.e5. doi: 10.1016/j.celrep.2018.12.044
19. Jung E, Alfonso J, Osswald M, Monyer H, Wick W, Winkler F. Emerging Intersections Between Neuroscience and Glioma Biology. *Nat Neurosci* (2019) 22(12):1951–60. doi: 10.1038/s41593-019-0540-y
20. Zarco N, Norton E, Quinones-Hinojosa A, Guerrero-Cazares H. Overlapping Migratory Mechanisms Between Neural Progenitor Cells and Brain Tumor Stem Cells. *Cell Mol Life Sci* (2019) 76(18):3553–70. doi: 10.1007/s00018-019-03149-7
21. Alcantara Llaguno S, Chen J, Kwon CH, Jackson EL, Li Y, Burns DK, et al. Malignant Astrocytomas Originate From Neural Stem/Progenitor Cells in a Somatic Tumor Suppressor Mouse Model. *Cancer Cell* (2009) 15(1):45–56. doi: 10.1016/j.ccr.2008.12.006
22. Alcantara Llaguno S, Sun D, Pedraza AM, Vera E, Wang Z, Burns DK, et al. Cell-of-Origin Susceptibility to Glioblastoma Formation Declines With Neural Lineage Restriction. *Nat Neurosci* (2019) 22(4):545–55. doi: 10.1038/s41593-018-0333-8
23. Duan S, Yuan G, Liu X, Ren R, Li J, Zhang W, et al. PTEN Deficiency Reprogrammes Human Neural Stem Cells Towards a Glioblastoma Stem Cell-Like Phenotype. *Nat Commun* (2015) 6:10068–. doi: 10.1038/ncomms10068
24. Jacques TS, Swales A, Brzozowski MJ, Henriquez NV, Linehan JM, Mirzadeh Z, et al. Combinations of Genetic Mutations in the Adult Neural Stem Cell Compartment Determine Brain Tumour Phenotypes. *EMBO J* (2010) 29(1):222–35. doi: 10.1038/emboj.2009.327
25. Lee JH, Lee JE, Kahng JY, Kim SH, Park JS, Yoon SJ, et al. Human Glioblastoma Arises From Subventricular Zone Cells With Low-Level Driver Mutations. *Nature* (2018) 560(7717):243–7. doi: 10.1038/s41586-018-0389-3
26. Bexell D, Gunnarsson S, Nordquist J, Bengzon J. Characterization of the Subventricular Zone Neurogenic Response to Rat Malignant Brain Tumors. *Neuroscience* (2007) 147(3):824–32. doi: 10.1016/j.neuroscience.2007.04.058
27. Galli R, Binda E, Orfanelli U, Cipelletti B, Gritti A, De Vitis S, et al. Isolation and Characterization of Tumorigenic, Stem-Like Neural Precursors From Human Glioblastoma. *Cancer Res* (2004) 64(19):7011–21. doi: 10.1158/0008-5472.CAN-04-1364
28. Abbadi S, Rodarte JJ, Abutaleb A, Lavell E, Smith CL, Ruff W, et al. Glucose-6-phosphatase is a Key Metabolic Regulator of Glioblastoma Invasion. *Mol Cancer Res: MCR* (2014) 12(11):1547–59. doi: 10.1158/1541-7786.MCR-14-0106-T
29. Chaichana KL, Guerrero-Cazares H, Capilla-Gonzalez V, Zamora-Berridi G, Achanta P, Gonzalez-Perez O, et al. Intra-Operatively Obtained Human Tissue: Protocols and Techniques for the Study of Neural Stem Cells. *J Neurosci Methods* (2009) 180(1):116–25. doi: 10.1016/j.jneumeth.2009.02.014
30. Gonzalez-Perez O, Guerrero-Cazares H, Quiñones-Hinojosa A. Targeting of Deep Brain Structures With Microinjections for Delivery of Drugs, Viral Vectors, or Cell Transplants. *J Vis Exp: JoVE* (2010) 46. doi: 10.3791/2082
31. Guerrero-Cazares H, Tzeng SY, Young NP, Abutaleb AO, Quinones-Hinojosa A, Green JJ. Biodegradable Polymeric Nanoparticles Show High Efficacy and Specificity at DNA Delivery to Human Glioblastoma *In Vitro* and *In Vivo*. *ACS nano* (2014) 8(5):5141–53. doi: 10.1021/nn501197v
32. Gundersen HJ, Jensen EB. The Efficiency of Systematic Sampling in Stereology and its Prediction. *J Microsc* (1987) 147(Pt 3):229–63. doi: 10.1111/j.1365-2818.1987.tb02837.x
33. Ellis P, Fagan BM, Magness ST, Hutton S, Taranova O, Hayashi S, et al. SOX2, a Persistent Marker for Multipotential Neural Stem Cells Derived From Embryonic Stem Cells, the Embryo or the Adult. *Dev Neurosci* (2004) 26(2-4):148–65. doi: 10.1159/000082134
34. Doetsch F, Garcia-Verdugo JM, Alvarez-Buylla A. Cellular Composition and Three-Dimensional Organization of the Subventricular Germinal Zone in the Adult Mammalian Brain. *J Neurosci: Off J Soc Neurosci* (1997) 17(13):5046–61. doi: 10.1523/JNEUROSCI.17-13-05046.1997
35. Kaneko N, Marin O, Koike M, Hirota Y, Uchiyama Y, Wu JY, et al. New Neurons Clear the Path of Astrocytic Processes for Their Rapid Migration in the Adult Brain. *Neuron* (2010) 67(2):213–23. doi: 10.1016/j.neuron.2010.06.018
36. Jafri NF, Clarke JL, Weinberg V, Barani IJ, Cha S. Relationship of Glioblastoma Multiforme to the Subventricular Zone is Associated With Survival. *Neuro Oncol* (2013) 15(1):91–6. doi: 10.1093/neuonc/nos268
37. Mistry AM, Wooten DJ, Davis LT, Mobley BC, Quaranta V, Ihrle RA. Ventricular-Subventricular Zone Contact by Glioblastoma is Not Associated With Molecular Signatures in Bulk Tumor Data. *Sci Rep* (2019) 9(1):1842. doi: 10.1038/s41598-018-37734-w
38. Steed TC, Treiber JM, Patel K, Ramakrishnan V, Merk A, Smith AR, et al. Differential Localization of Glioblastoma Subtype: Implications on Glioblastoma Pathogenesis. *Oncotarget* (2016) 7(18):24899–907. doi: 10.18632/oncotarget.8551
39. Steed TC, Treiber JM, Taha B, Engin HB, Carter H, Patel KS, et al. Glioblastomas Located in Proximity to the Subventricular Zone (SVZ) Exhibited Enrichment of Gene Expression Profiles Associated With the Cancer Stem Cell State. *J Neuro-Oncol* (2020) 148(3):455–62. doi: 10.1007/s11060-020-03550-4
40. Carrano A, Zarco N, Phillipps J, Lara-Velazquez M, Suarez-Meade P, Norton ES, et al. Human Cerebrospinal Fluid Modulates Pathways Promoting Glioblastoma Malignancy. *Front Oncol* (2021) 11(502). doi: 10.3389/fonc.2021.624145
41. Lara-Velazquez M, Zarco N, Carrano A, Phillipps J, Norton ES, Schiapparelli P, et al. Alpha 1-Antichymotrypsin Contributes to Stem Cell Characteristics and Enhances Tumorigenicity of Glioblastoma. *Neuro Oncol* (2021) 23(4):599–610. doi: 10.1093/neuonc/noaa264
42. Qin EY, Cooper DD, Abbott KL, Lennon J, Nagaraja S, Mackay A, et al. Neural Precursor-Derived Pleiotrophin Mediates Subventricular Zone Invasion by Glioma. *Cell* (2017) 170(5):845–59.e19. doi: 10.1016/j.cell.2017.07.016
43. Sawamoto K, Wichterle H, Gonzalez-Perez O, Cholfin JA, Yamada M, Spassky N, et al. New Neurons Follow the Flow of Cerebrospinal Fluid in the Adult Brain. *Sci (New York NY)* (2006) 311(5761):629–32. doi: 10.1126/science.1119133
44. Duntsch C, Zhou Q, Weimar JD, Frankel B, Robertson JH, Pourmotabbed T. Up-Regulation of Neurogenesis Generating Glial Progenitors That Infiltrate Rat Intracranial Glioma. *J Neuro-Oncol* (2005) 71(3):245–55. doi: 10.1007/s11060-004-2156-6

45. Cantanhede IG, de Oliveira JRM. Pdgf Family Expression in Glioblastoma Multiforme: Data Compilation From Ivy Glioblastoma Atlas Project Database. *Sci Rep* (2017) 7(1):15271. doi: 10.1038/s41598-017-15045-w
46. Jackson EL, Garcia-Verdugo JM, Gil-Perotin S, Roy M, Quinones-Hinojosa A, VandenBerg S, et al. PDGFR Alpha-Positive B Cells are Neural Stem Cells in the Adult SVZ That Form Glioma-Like Growths in Response to Increased PDGF Signaling. *Neuron* (2006) 51(2):187–99. doi: 10.1016/j.neuron.2006.06.012
47. Bruggeman SW, Hulsman D, Tanger E, Buckle T, Blom M, Zevenhoven J, et al. Bmi1 Controls Tumor Development in an Ink4a/Arf-independent Manner in a Mouse Model for Glioma. *Cancer Cell* (2007) 12(4):328–41. doi: 10.1016/j.ccr.2007.08.032
48. Lawlor K, Marques-Torrejon MA, Dharmalingham G, El-Azhar Y, Schneider MD, Pollard SM, et al. Glioblastoma Stem Cells Induce Quiescence in Surrounding Neural Stem Cells Via Notch Signalling. *Genes Dev* (2020) 34(23–24):1599–604. doi: 10.1101/gad.336917.120
49. Suh H, Consiglio A, Ray J, Sawai T, D'Amour KA, Gage FH. In Vivo Fate Analysis Reveals the Multipotent and Self-Renewal Capacities of Sox2+ Neural Stem Cells in the Adult Hippocampus. *Cell Stem Cell* (2007) 1(5):515–28. doi: 10.1016/j.stem.2007.09.002
50. Walton C, Pariser E, Nottebohm F. The Zebra Finch Paradox: Song is Little Changed, But Number of Neurons Doubles. *J Neurosci: Off J Soc Neurosci* (2012) 32(3):761–74. doi: 10.1523/JNEUROSCI.3434-11.2012
51. Codega P, Silva-Vargas V, Paul A, Maldonado-Soto AR, Deleo AM, Pastrana E, et al. Prospective Identification and Purification of Quiescent Adult Neural Stem Cells From Their *In Vivo* Niche. *Neuron* (2014) 82(3):545–59. doi: 10.1016/j.neuron.2014.02.039
52. Petrik D, Myoga MH, Grade S, Gerkau NJ, Pusch M, Rose CR, et al. Epithelial Sodium Channel Regulates Adult Neural Stem Cell Proliferation in a Flow-Dependent Manner. *Cell Stem Cell* (2018) 22(6):865–78.e8. doi: 10.1016/j.stem.2018.04.016
53. Ma Q, Schlegel F, Bachmann SB, Schneider H, Decker Y, Rudin M, et al. Lymphatic Outflow of Cerebrospinal Fluid is Reduced in Glioma. *Sci Rep* (2019) 9(1):14815. doi: 10.1038/s41598-019-51373-9
54. Tirapelli LF, Bolini PH, Tirapelli DP, Peria FM, Becker AN, Saggiaro FP, et al. Caspase-3 and Bcl-2 Expression in Glioblastoma: An Immunohistochemical Study. *Arquivos Neuropsiquiatr* (2010) 68(4):603–7. doi: 10.1590/S0004-282X2010000400023

Conflict of Interest: The authors declare that the research was conducted in the absence of any commercial or financial relationships that could be construed as a potential conflict of interest.

Copyright © 2021 Ripari, Norton, Bodoque-Villar, Jeanneret, Lara-Velazquez, Carrano, Zarco, Vazquez-Ramos, Quiñones-Hinojosa, de la Rosa-Prieto and Guerrero-Cázares. This is an open-access article distributed under the terms of the Creative Commons Attribution License (CC BY). The use, distribution or reproduction in other forums is permitted, provided the original author(s) and the copyright owner(s) are credited and that the original publication in this journal is cited, in accordance with accepted academic practice. No use, distribution or reproduction is permitted which does not comply with these terms.